ACS Catalysis

Research Article

pubs.acs.org/acscatalysis

Cp*Ir^{III}-Catalyzed Oxidative Coupling of Benzoic Acids with Alkynes

Daniel A. Frasco, Cassandra P. Lilly, Paul D. Boyle, and Elon A. Ison*

Department of Chemistry, North Carolina State University, 2620 Yarbrough Drive, Raleigh, North Carolina 27695-8204, United States

Supporting Information

ABSTRACT: Cp*Ir(III) complexes have been shown to catalyze the oxidative coupling of benzoic acids with alkynes in methanol at 60 °C to form a variety of isocoumarins. The use of AgOAc as an oxidant was required to facilitate significant product formation. Alkyl alkynes were shown to be more reactive substrates than aryl alkynes, and a number of functional groups were tolerated on benzoic acid. Combined mechanistic and computational studies (BP86) revealed that (1) C−H activation occurs via an acetate-assisted mechanism; (2) C−H activation is not turnover limiting; and (3) the oxidant oxidizes the reduced form of the catalyst via an Ir(I)−Ir(II)−Ir(III) sequence.

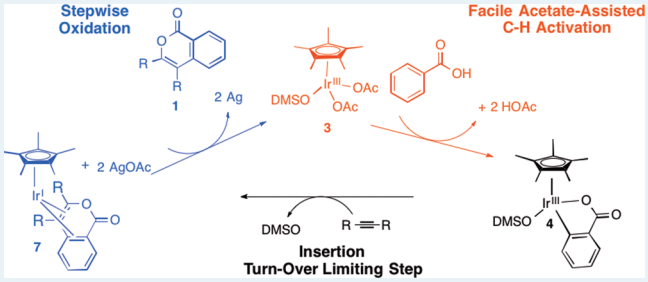

KEYWORDS: *C−H functionalization, oxidative coupling, C−H activation, Cp*Ir^{III}, annulation*

INTRODUCTION

Isocoumarins are important components in many natural products. They show a broad range of biological activity including antifungal,[1] antiulcer,[2] anti-inflamatory,[3] antibacterial,[4] herbicidal,[5] cytotoxic,[6] and antiangiogenic[7] applications. Isocoumarins also function as key intermediates in the synthesis of a variety of other compounds including isoquinolines, isochromenes, and isocarbostyrils.[8] In many cases, isocoumarins are synthesized from the intramolecular cyclization of substrates that contain both an alkyne and a carboxylate group. However, these reactions often require multiple steps to generate the starting material, halogen functionalized reagents, or the stoichiometric use of transition metals.[3,8−13] Some of these reactions also result in a number of undesired side products and many show poor atom economy.[8−11]

In recent years there has been significant interest in the transition-metal catalyzed oxidative annulations[14−17] of alkynes with carboxylic acids. For example, Ackermann and co-workers have recently shown that cationic ruthenium(II) catalysts enabled the synthesis of isocoumarins through the oxidative coupling of alkynes with benzoic acids.[18] In addition, Jeganmohan and co-workers reported high regioselectivity for the oxidative cyclization of aromatic acids with alkynes in the presence of catalytic amounts of cationic ruthenium(II) catalysts to provide highly substituted isocoumarin derivatives.[19]

In addition to catalysis with ruthenium(II) complexes,[20−36] Miura, Satoh and co-workers have pioneered catalysis with rhodium and iridium.[37−41] For example, it was demonstrated that rhodium(III) catalysts in the presence of copper salts were effective in the oxidative annulation of alkynes with benzoic acids. Interestingly, when iridium(III) catalysts were used in the presence of silver salts for the same reaction, the desired isocoumarins were not formed. Instead, the oxidative annulation reaction lead to the formation of substituted napthalenes.[42] In previous work from our lab, we showed that Cp*Ir^{III} complexes were capable of catalytic C−H activation of benzoic acid via H/D exchange studies, and that these catalysts were also capable of functionalization, as benzoquinone insertion resulted in the formation of benzochromenones.[43]

Despite the recent flurry of studies dealing with the catalytic oxidative annulation of alkynes with benzoic acids, there have been limited investigations aimed at understanding the reaction mechanism. Further, while Cp*Ir^{III} complexes have been among the most effective in stoichiometric C−H activation reactions,[44] catalytic oxyfunctionalization with these species has been much less developed.[45−50] In addition, the tendency of third row transition metals to form complexes that are more stable than their first and second row analogues allows for the isolation or identification of species that may be important intermediates in the catalytic cycle.

In this work, we report conditions for the iridium-catalyzed synthesis of isocoumarins from benzoic acids and alkynes. In addition, we investigate the mechanism for the reaction. As a result of this study, we have addressed questions that remain in the transition-metal catalyzed annulation of alkynes with benzoic acids. Specifically, we address the following questions: (1) What is the mechanism for the C−H activation step in these reactions? (2) What is the turnover-limiting step for these reactions, C−H activation or C−H functionalization? (3) What is the role of the external oxidant in these reactions? Our

Received: August 7, 2013
Revised: September 5, 2013
Published: September 9, 2013

   dx.doi.org/10.1021/cs400656q | ACS Catal. 2013, 3, 2421−2429

mechanistic insight should aid in the development of appropriate catalysts for the annulation of alkynes with benzoic acids, and, more broadly, for catalytic C−H functionalization reactions.

RESULTS AND DISCUSSION

Reaction Optimization. Previously, Miura and Satoh reported that the iridium catalyzed annulation of alkynes with benzoic acids resulted in the formation of substituted napthalenes, instead of isocoumarins, that were observed with the analogous rhodium catalysts.[42,51] However, we have been able to discover conditions for the successful formation of isocoumarins (vide infra).

The optimal conditions for the formation of 3,4-diphenylisocoumarin, **1a**, from benzoic acid and diphenylacetylene in methanol are shown in Scheme 1. Reaction yields were determined by ^{1}H NMR spectroscopy with an internal standard (Supporting Information, Table S1).

Scheme 1. Catalytic Formation of 3,4-Diphenylisocoumarin, 1a, from Benzoic Acid and Diphenylacetylene

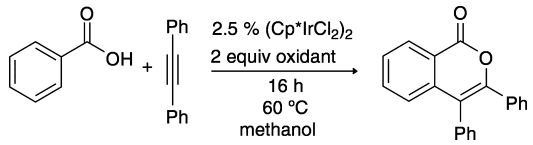

A variety of oxidants were investigated for their compatibility in this reaction including AgOAc, $Cu(OAc)_2$, $AgNO_3$, Ag_2O, AgO_2CCF_3, and Ag_2CO_3. AgOAc was found to be the most effective oxidant. Other Ir(III) catalysts were examined for this reaction, and most exhibited similar reactivity to $(Cp^*IrCl_2)_2$ (See Supporting Information).

Substrate Scope. The optimal reaction conditions for the synthesis of **1a** were utilized for a variety of alkynes with the exception that the reaction time was increased to 24 h to maximize conversion. The isolated yields for a number of isocoumarins using aryl-alkynes as substrates are reported in Scheme 2. Substrates with substituents in the *para* position of benzoic acid, as well the *para* position of diphenylacetylene are tolerated in this reaction.

When alkyl-alkynes were used instead of the more sterically hindered aryl-alkynes yields significantly increased (Scheme 3).

Scheme 2. Synthesis of Isocoumarins from Aryl Alkynes

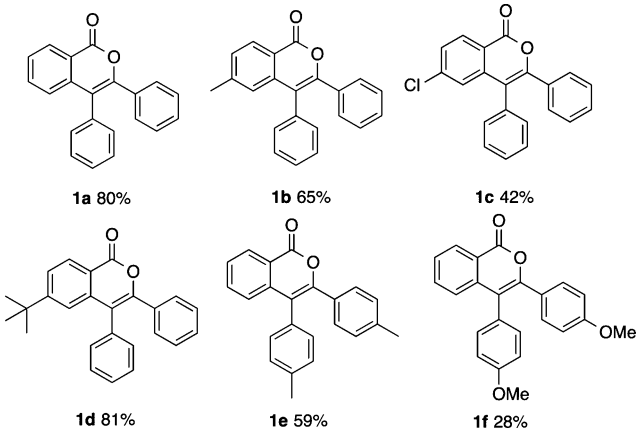

.

Scheme 3. Synthesis of Isocoumarins from Alkyl Alkynes

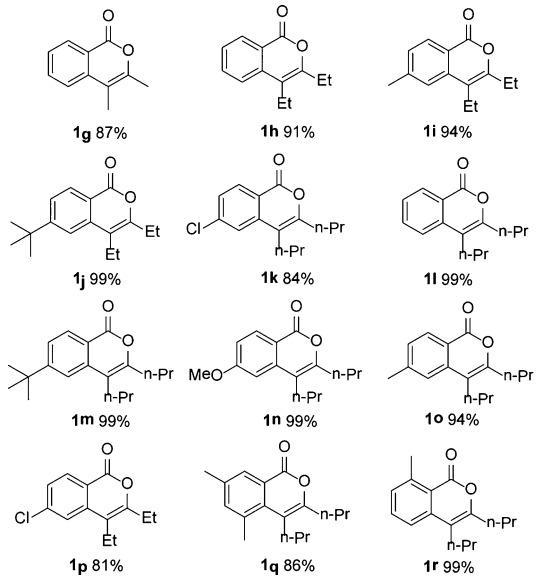

Like the reactions with aryl alkynes, electron withdrawing and electron donating groups are also tolerated in this reaction. Benzoic acids with methyl groups at the *meta* and *ortho*-positions were also effective (**1q−1r**).

We have also examined the reaction of unsymmetrical alkynes in this system. While the reaction did not proceed with the terminal alkyne, phenylacetylene, regioselective isocoumarin formation was observed when 1-phenyl-1-propyne and 1-phenyl-1-pentyne were employed as substrates (See Supporting Information). For example, the reaction with 1-phenyl-1-propyne afforded the regioisomeric isocoumarin derivative **1s**, where the alkyne carbon bearing the phenyl group is attached to the carboxylate group of benzoic acid, and the alkyne carbon bearing the alkyl group is connected to the ortho carbon. The minor regioisomer **1s′** was also formed in the reaction where the phenyl group of the alkyne is now attached to the ortho carbon of the benzoic acid and the alkyl group is attached to the carboxylate group. These isocoumarins formed in a 14:1 ratio. Similarly, when 1-phenyl-1-pentyne was used as a substrate, the corresponding regioisomers, **1t** and **1t′**, were formed in an approximately 6:1 ratio. Although we have not optimized the current system for regioselectivity, the reactivity seen here is comparable to the catalytic system reported by Jeganmohan and co-workers.[19]

Mechanistic Analysis. Although the coupling of benzoic acids with alkynes to form isocoumarins has been examined with other transition metals, little work has been done to understand the mechanism. To simplify mechanistic studies, $Cp^*Ir(Me_2SO)Cl_2$, **2**, was synthesized as shown in Scheme 4.[52] This catalyst exhibited similar reactivity to $(Cp^*IrCl_2)_2$.

Treatment of **2** with AgOAc in dry benzene for 2 h afforded the bis-acetate complex $Cp^*Ir(Me_2SO)(OAc)_2$, **3** (Scheme 4). This acetate complex was characterized by ^{1}H, ^{13}C NMR spectroscopy, IR spectroscopy, elemental analysis, and X-ray crystallography (See Supporting Information). X-ray quality crystals were obtained by slow diffusion of pentane into a concentrated solution of **3** in dichloromethane as shown in Scheme 4. The geometry about the metal center can be described as a piano stool with two equivalent monodentate acetate ligands.

dx.doi.org/10.1021/cs400656q | ACS Catal. 2013, 3, 2421−2429

Scheme 4. Synthesis of Complexes 2 and 3

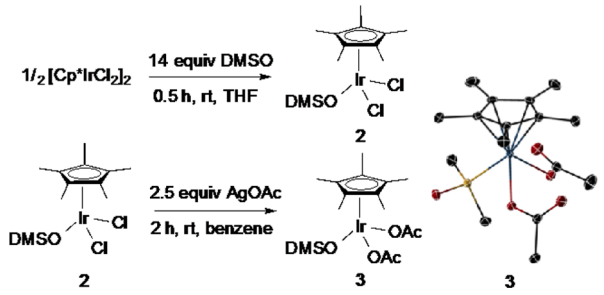

Recently the mechanism for C−H activation for catalysts that contain acetate ligands has been proposed to proceed by an acetate-assisted mechanism.[53−57] A similar mechanism may be proposed for the C−H activation step in this catalytic cycle (Scheme 5). In this mechanism, complex **3** reacts with benzoic

Scheme 5. Proposed Mechanism for Isocoumarin Formation

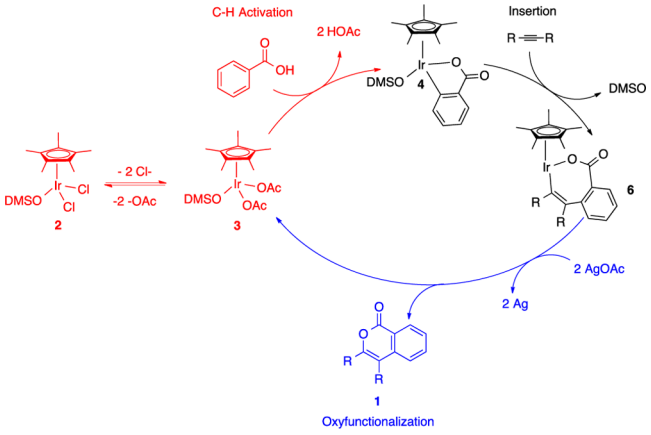

acid through an acetate assisted C−H activation reaction to form an iridium metallacycle **4**. Insertion of an alkyne into **4** results in metallacycle **6**. Subsequently, oxidant-induced oxyfunctionalization results in the formation of the isocoumarin product. We have examined each of the steps in the proposed mechanism in detail.

1. C−H Activation. The stoichiometric reaction at room temperature of **3** with 1 equiv of benzoic acid for 24 h resulted in the formation of the cyclometalated benzoate complex, $Cp^*Ir(Me_2SO)(O_2CC_6H_4)$, **4a**. Under conditions similar to the catalytic reaction, (60 °C), complex **4a** was formed in approximately 1 h (Scheme 6).

When similar reactions were attempted with $(Cp^*IrCl_2)_2$ and $Cp^*Ir(Me_2SO)Cl_2$, **2**, no reaction was observed. It is also worth noting that the formation of **4a** from **3** was not reversible. In the presence of excess acetic acid (10 equiv), **4a** was not converted to **3** at room temperature for 24 h.

Substituted benzoic acids reacted with **3** to form a variety of cyclometalated iridium complexes (**4b**−**4f**). The substituent in the *para* position did not seem to affect product yields as all complexes were formed with near quantitative yields after 1 h at 60 °C. Complexes **4b**−**4f** have been characterized by ^1H, ^{13}C NMR spectroscopy, IR spectroscopy, elemental analysis, and X-ray crystallography (See Supporting Information). The representative crystal structure of **4e** is shown Scheme 6.

The facile formation of **4** from **3** at mild conditions and in high yields suggest that C−H activation is not turnover limiting

Scheme 6. Synthesis of Complex 4

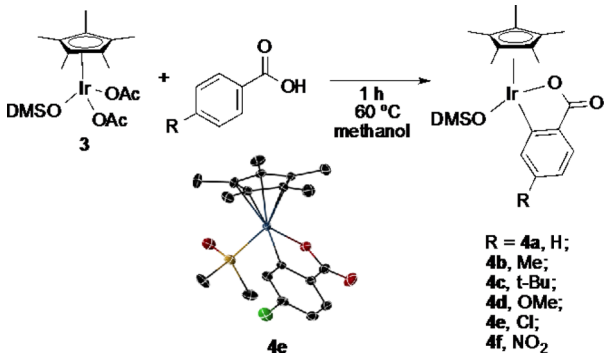

for the catalytic reaction. Significantly, the formation of **4** is complete in 1 h. In contrast, the catalytic reactions require around 10−24 h for complete conversion. In addition, the observation that complexes lacking acetate ligands like **2** and $(Cp^*IrCl_2)_2$ do not result in the formation of **4** strongly suggests that **3** or a related acetate species formed in situ are important intermediates for the formation of isocoumarin, and that the acetate ligand is critical in promoting C−H activation.

2. Alkyne Insertion Step. The viability of **4a** as an intermediate in the catalytic cycle was also investigated. When **4a** was used as a catalyst, comparable reactivity to $(Cp^*IrCl_2)_2$ was observed which suggests **4a** is a catalytically competent species. As a result, catalyst **4a** was used to study the insertion step in the catalytic cycle depicted in Scheme 5.

When **4a** was treated with 4-octyne in the absence of AgOAc, for 2 h, four new peaks in the aromatic region were observed in the ^1H NMR spectrum at 7.20 (dd, 1H), 6.92 (dd, 1H), 6.88 (ddd, 1H), and 6.63 ppm (ddd, 1H) (Figure 1b). After 24 h,

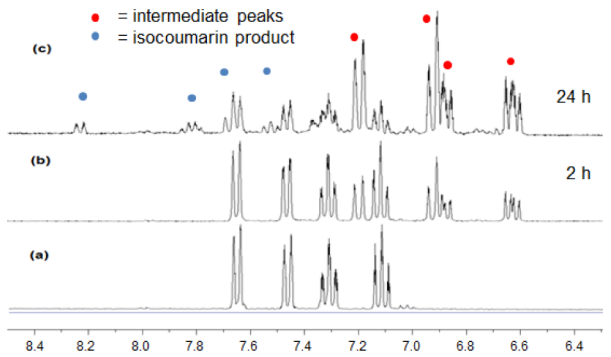

Figure 1. ^1H NMR spectrum (aromatic region) for the reaction of 4-octyne with **4a** at 60 °C: (a) **4a** and 4-octyne at room temperature; (b) **4a** and 4-octyne after heating at 60 °C for 2 h; (c) **4a** and 4-octyne after heating at 60 °C for 24 h.

these resonances increased and the peaks for **4a** decreased (Figure 1c). Small peaks corresponding to the final product 3,4-dipropylisocoumarin were also observed at 8.23 ppm, 7.83 ppm, 7.68 ppm, and 7.52 ppm.

We considered three possibilities for the identity of the intermediate observed in the reactions in Figure 1: the alkyne complex $Cp^*Ir^{III}(C_8H_{14})(O_2CC_6H_4)$, **5l**, with 4-octyne replacing dimethylsulfoxide (DMSO) as the neutral ligand coordinated to the metal, $Cp^*Ir^{III}(O_2CC_6H_4C_8H_{14})$, **6l**, where the alkyne inserted into the Ir−C bond in **4a**, or $Cp^*Ir^{I}(O_2CC_6H_4C_8H_{14})$, **7l**, where reductive elimination of a C−O bond results in an Ir(I) complex (Scheme 7). It should be

dx.doi.org/10.1021/cs400656q | ACS Catal. 2013, 3, 2421−2429

noted that free DMSO was observed in the reaction of **4a** with 4-octyne, which would indicate that DMSO was not bound to the metal in the intermediate.

Scheme 7. Proposed Intermediates for Alkyne Insertion Step

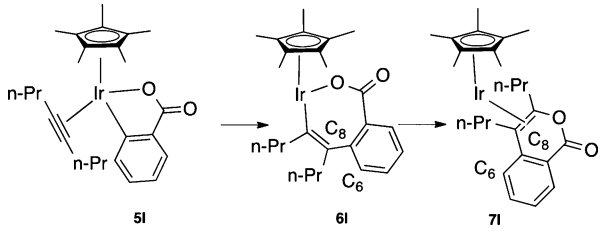

A variety of 2D NMR experiments were performed to determine the identity of the intermediate. If **6l** or **7l** were the intermediate, long-range coupling between the C8 alkyne carbon with aromatic protons from the benzoate rings at C6 would be expected in an HMBC experiment. In contrast, long-range coupling between the alkyne carbons and the benzoate ring would not be expected in **5l** as the proton on the benzoate ring is 4 bonds away.

In the HMBC spectrum from 51 ppm−101 ppm long-range coupling was observed between the four new aromatic protons and the new quaternary carbons at 56.7 ppm, 67.5 ppm, and 87.0 ppm (See Supporting Information). The peak at 67.5 ppm was assigned as C8 because of its three bond coupling with the proton on C6 at 7.10 ppm. This coupling would rule out **5l** as the observed intermediate.

3. Oxyfunctionalization. The effect of an oxidant in the stoichiometric insertion of an alkyne with **4a** and subsequent oxyfunctionalization to form **1a** was examined (Table 1). Minimal product formation was observed for the reaction of diphenylacetylene with **4a** in the absence of an additive, (Entry 1). However, when 2 equiv of AgOAc were added to the reaction, **1a** was formed in 75% yield (Entry 2). Both sodium acetate and acetic acid were used as additives to determine the effect of the acetate anion in the absence of an oxidant (Entries 3−4). Neither of these produced a significant amount of **1a**. The oxidants Ag_2CO_3 and Ag_2O were also used and resulted in 54% and 16% yields respectively (Entries 5−6).

Table 1. Stoichiometric Reactions of 4a with Diphenylacetylene and a Variety of Additives

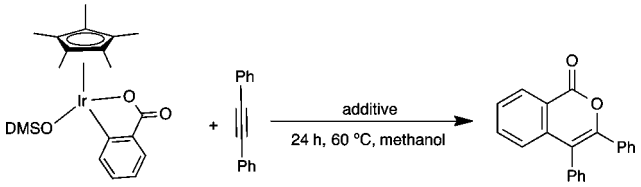

entry	additive	% yield **1**[a]
1	none	5(1)
2	AgOAc	75(1)
3	NaOAc	ND[b]
4	HOAc	12(1)
5	Ag_2CO_3	54(1)
6	Ag_2O	16(3)

[a]Reaction conditions: 26 mg (0.05 mmol) of **4a**, 9 mg (0.05 mmol) of diphenylacetylene, and (0.10 mmol) of an additive in 1 mL of methanol under air, in triplicate. Errors are standard deviations of the mean. Percent yield determined by crude NMR versus an internal standard. [b]No product was detected.

The data presented above suggest that an oxidant is required for significant product formation. The specific role of the oxidant in the insertion and reductive elimination steps was investigated with 4-octyne because the catalytic reaction proceeded at a faster rate (10 h as opposed to 24 h) with this alkyne, and the lack of aromatic protons allowed for simplification of the ^{1}H NMR spectrum.

In a storage tube, **4a** and 4-octyne were heated at 60 °C for 4 h in methanol. The expected mixture of **4a** and the previously observed intermediate was observed (see Figure 1). Two equivalents of AgOAc were then added to this reaction mixture. An analysis after 1 h revealed that peaks for the intermediate were no longer present, and peaks for **1l** greatly increased (Scheme 8). The only other significant aromatic peaks remaining in the spectrum were from unreacted **4a**.

Scheme 8. Sequential Reactions of 4a with 4-Octyne and AgOAc

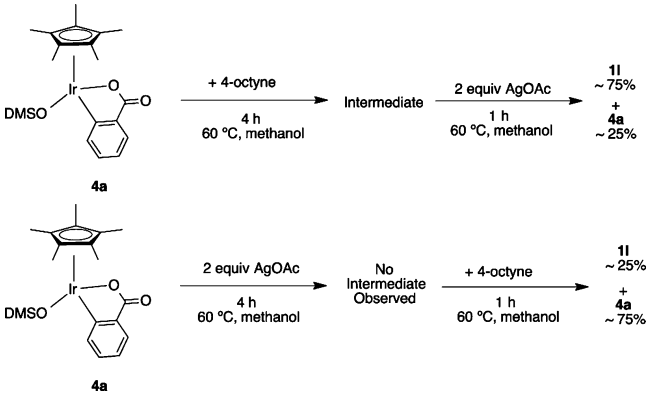

When **4a** and AgOAc were heated at 60 °C for 4 h, no obvious intermediate was observed, and it appeared that **4a** remained unreacted.[58] Upon adding 4-octyne, the production of **1l** was sluggish; after 1 h, the aromatic region was primarily composed of unreacted **4a** and a minimal amount of **1l** (Scheme 8). When this reaction mixture was allowed to stir for 24 h, significant peaks for **1l** were observed, but all components of the catalytic reaction were present under these conditions.

We propose that the intermediate observed in the absence of AgOAc is the Ir(I) complex, **7**. The addition of AgOAc quickly regenerates the Ir(III) active catalyst and releases the isocoumarin product. *The formation of 7 occurs slowly over time. However, once AgOAc is added, isocoumarin is quickly formed.*

Recently, Huang and co-workers[59] reported that an analogous Rh(I) intermediate was isolated in oxidative C−H activation/annulation reactions. Upon addition of an oxidant, the cyclometalated product was released, and the active Rh(III) catalyst was regenerated.

The observation of minimal isocoumarin formation in Scheme 8 when **4a** was reacted initially with AgOAc for 4 h, followed by the addition of 4-octyne, is likely because the concentration of **7** is low under these conditions. These results are consistent with the proposed mechanism in Scheme 5. The role of the oxidant in the oxyfunctionalization step was further examined computationally.

dx.doi.org/10.1021/cs400656q | *ACS Catal.* 2013, 3, 2421−2429

Computational Mechanistic Analysis. Density functional theory (DFT) calculations (BP86) were conducted to elaborate on our experimental observations, as well as to address unanswered questions, such as the role of the oxidant in the catalytic cycle as described above. The proposed mechanism for isocoumarin formation was divided into 3 key steps: C−H activation, insertion, and oxyfunctionalization.

C−H activation. Two mechanisms were considered for the C−H activation step: an oxidative addition mechanism and an acetate assisted mechanism (Scheme 9). The mechanism for

Scheme 9. DFT(BP86) Computed Pathways for C−H Activation[a]

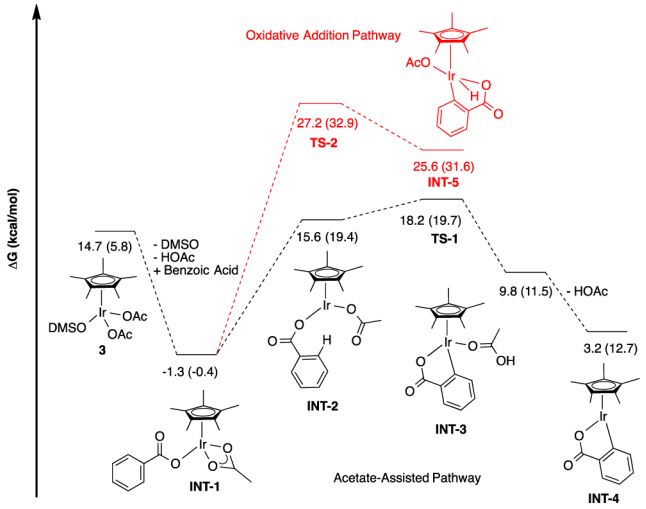

[a]All energies are relative to Cp*Ir(OAc)$_2$ + benzoic acid + DMSO + $Ag_2(OAc)_2$ which was set to 0.0 kcal/mol. Values in parentheses are gas phase energies.

C−H activation with complexes incorporating acetate ligands has been extensively studied.[53,60−64] These studies suggest that the acetate ligand acts as an internal base and plays a critical role in activating the C−H bond. As mentioned previously, the formation of **4** from **3** and benzoic acid takes place in 1 h at 60 °C.

Oxidative addition of the C−H bond at the Ir center to form an Ir(V) hydride complex proceeds through **TS-2 to INT-5** with an activation barrier of 27.2 kcal/mol. The reaction is endergonic overall (ΔG° = 25.6 kcal/mol). The high energy of this Ir(V) intermediate suggests that the oxidative addition pathway is unlikely.[65]

An acetate-assisted mechanism was also considered. Addition of benzoic acid and loss of DMSO and HOAc results in the formation of **INT-1** (ΔG° = −1.3 kcal/mol). Rotation of the benzoate ligand and κ^2 to κ^1 displacement of the acetate ligand gives **INT-2** (ΔG° = 15.6 kcal/mol). In this intermediate, the ortho hydrogen atom on the benzoate ring interacts with the acetate ligand with a bond distance of 1.74 Å. Activation of the C−H bond occurs via **TS-1** ($\Delta G^\ddagger$ = 18.2 kcal/mol) whose structure and selected bond lengths are depicted in Figure 2. The bond lengths in **TS-1** are similar to Ir(III) complexes that have been reported to operate by an acetate-assisted mechanism. For example, Ess and co-workers reported similar bond lengths for the transition state for acetate-assisted C−H activation with an $(acac)_2Ir(OAc)$ complex.[66]

Proton transfer to the acetate ligand results in **INT-3** (ΔG° = 9.8 kcal/mol). This is followed by loss of acetic acid to produce

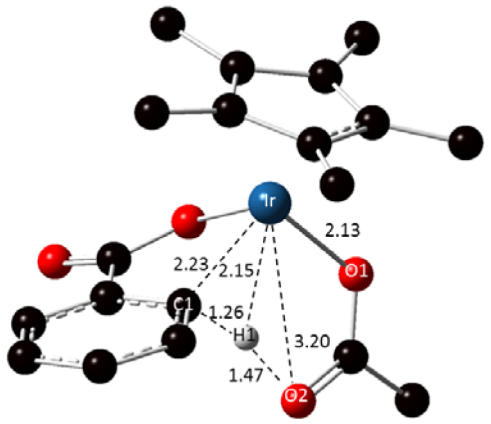

Figure 2. Structure for TS-1. Selected bond lengths in Å.

INT-4 (ΔG° = 3.2 kcal/mol). *These results suggest that the overall pathway for C−H activation via an acetate-assisted mechanism is significantly lower than the oxidative addition pathway.* Importantly, these results are consistent with experimental observations that acetate ligands are important for significant catalytic turnover.

Insertion. The mechanism for the insertion of alkynes into **INT-4** is depicted in Scheme 10. The insertion step was

Scheme 10. DFT(BP86) Computed Pathways for Insertion[a]

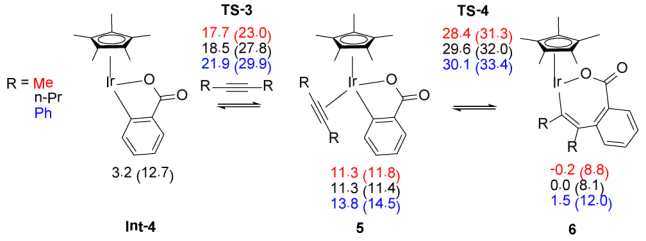

[a]All energies are relative to Cp*Ir(OAc)$_2$ + benzoic acid + DMSO + $Ag_2(OAc)_2$ which was set to 0.0 kcal/mol. Values in parentheses are gas phase energies.

analyzed with 3 different alkynes: 2-butyne, 4-octyne, and diphenylacetylene. Coordination of the alkyne proceeds through **TS-3** ($\Delta G^\ddagger$ = 17.7 kcal/mol, 2-butyne; 18.5 kcal/mol, 4-octyne; 21.9 kcal/mol, diphenylacetylene), to produce **5**, (ΔG° = 11.3 kcal/mol, 2-butyne; 11.3 kcal/mol, 4-octyne; 13.8 kcal/mol, diphenylacetylene). This is followed by insertion of the alkyne through **TS-4** ($\Delta G^\ddagger$ = 28.4 kcal/mol, 2-butyne; 29.6 kcal/mol, 4-octyne; 30.1, kcal/mol, diphenylacetylene) to produce **6** (ΔG° = −0.2 kcal/mol, 2-butyne; 0.0 kcal/mol, 4-octyne; 1.5 kcal/mol, diphenyl acetylene).

These results are consistent with the observation that alkyl alkynes resulted in higher yields of isocoumarins after 24 h than the corresponding aryl alkynes. The barriers for the coordination and insertion of diphenyl acetylene are the highest for the three alkynes considered. In addition, the formation of **5** and **6** is the most endergonic for this alkyne. These results would seem to indicate that smaller alkynes are better substrates for this reaction than larger alkynes, likely because of the steric interaction between the R group and benzoic acid phenyl ring in the transition state (Supporting Information, Figure S8).

Oxyfunctionalization. A number of computational pathways were analyzed for the oxyfunctionalization step (Scheme 11).[67] We first considered a mechanism where the Ir(III)

dx.doi.org/10.1021/cs400656q | ACS Catal. 2013, 3, 2421−2429

Scheme 11. DFT(BP86) Computed Pathways for Oxyfunctionalization[a]

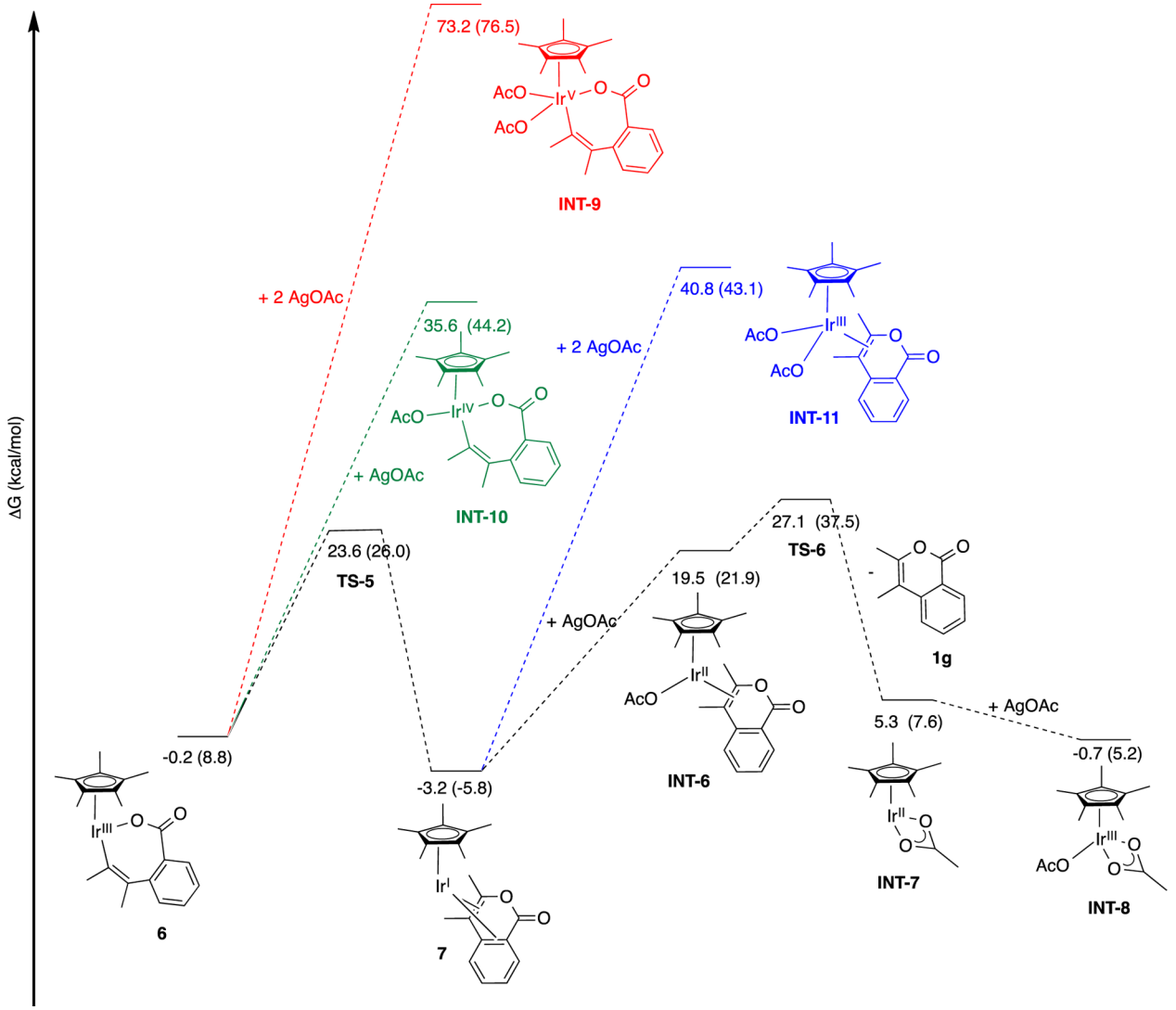

[a]All energies are relative to Cp*Ir(OAc)$_2$ + benzoic acid + DMSO + Ag$_2$(OAc)$_2$ which was set to 0.0 kcal/mol. Values in parentheses are gas phase energies.

Scheme 12. Calculated (BP86) Pathway for the Catalytic Formation of 1g[a]

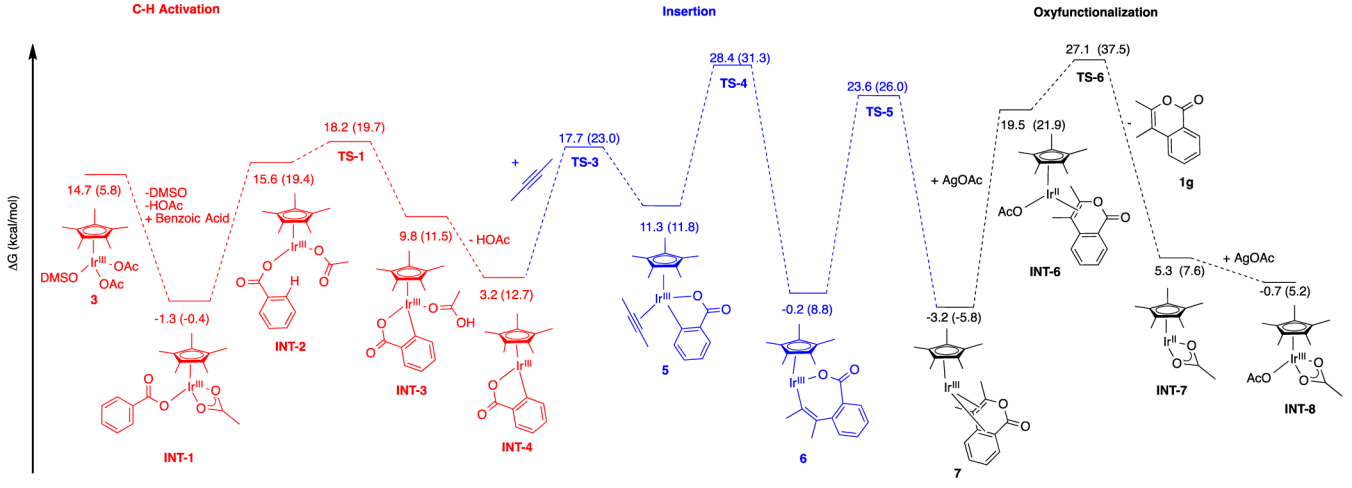

[a]All energies are relative to Cp*Ir(OAc)$_2$ + benzoic acid + DMSO + Ag$_2$(OAc)$_2$ which was set to 0.0 kcal/mol. Values in parentheses are gas phase energies..

dx.doi.org/10.1021/cs400656q | ACS Catal. 2013, 3, 2421−2429

complex **6** was first oxidized with 2 equiv of AgOAc to the Ir(V) complex, **INT-9**. The direct oxidation with silver acetate to Ir(V) is extremely endergonic (ΔG° = 73.2 kcal/mol) and as a result, this pathway is unlikely to be valid. Other Ir(V) pathways were considered, but these pathways were also endergonic (See Supporting Information).

The stepwise oxidation from Ir(III) to Ir(IV) was also considered, but this also resulted in the unfavorable formation **INT-10** (ΔG° = 35.6 kcal/mol).

In contrast, the reductive elimination from Ir(III) to Ir(I) followed by oxidation of Ir(I) to Ir(III) by AgOAc proved to be the most likely pathway. Reductive elimination from **6** proceeds through **TS-5**, ($\Delta G^\ddagger$ = 23.6 kcal/mol), to produce **7**, (ΔG° = −3.2 kcal/mol). *These results are also consistent with our proposal that* **7** *is the most likely intermediate that was observed when* ***4a*** *was reacted with an alkyne in the absence of AgOAc (vide supra).*

The oxidation of the Ir(I) complex, **7**, with AgOAc to regenerate the Ir(III) catalyst was examined next. The oxidation of **7** with 2 equiv of AgOAc to produce **INT-11** was found to be unfavorable (ΔG° = 40.8 kcal/mol). In contrast, the stepwise oxidation of **7** using sequential equivalents of AgOAc was found to be more favorable. This pathway proceeds from **7** to the Ir(II) complex, **INT-6**, (ΔG° = 19.5 kcal/mol). This complex then loses the isocoumarin product, **1g**, through **TS-6** ($\Delta G^\ddagger$ = 27.1 kcal/mol) to produce **INT-7** (ΔG° = 5.3 kcal/mol). This is followed by the oxidation of **INT-7** with an equivalent of AgOAc to generate **INT-8** (ΔG° = −0.7 kcal/mol). Various other reductive elimination pathways were also considered but resulted in unreasonable energy values (Supporting Information).

The overall energy diagram for the catalytic reaction using benzoic acid and 2-butyne as a substrate is depicted in Scheme 12. The turnover-limiting step is the insertion of 2-butyne. This is consistent with experimental observations as bulkier aryl-alkynes were shown to result in lower yields of isocoumarins than the corresponding alkyl-alkynes after 24 h.

CONCLUSIONS

In this paper, we have found conditions for the successful synthesis of isocoumarins from alkynes and benzoic acids using Cp*Ir^{III} catalysts. The reaction occurs at relatively mild conditions (60 °C, 24 h in CH_3OH), and requires AgOAc as an oxidant. We were able to determine through a series of experimental and computational studies that (1) C−H activation in this catalytic system most likely proceeds by an acetate-assisted mechanism, with the acetate ligand playing a critical role in cleaving the C−H bond in benzoic acid; (2) the turn over limiting step for the catalytic reaction is alkyne insertion and not C−H activation as proposed in some other systems;[14] and (3) oxyfunctionalization in this catalytic system is facile and the oxidant regenerates the active catalyst to its active oxidation state Ir(III). Interestingly, the oxidant does this in a stepwise manner by first oxidizing Ir(I) to Ir(II) followed by the oxidation of Ir(II) to Ir(III).

In recent years Cp*Ir^{III} complexes have become popular as catalysts for a variety of oxidation[45−47] and hydroxylation reactions.[48−50] These systems often require large equivalents of harsh oxidants and are often performed under forcing conditions. Recently, many of these systems have been shown to involve nanoparticles or other colloidal species.[68] In other cases, the generation of high-valent Ir species results in the displacement or transformation of the Cp* ligand to generate new catalytic species.[47,69] Here we have shown that under mild conditions, Cp*Ir^{III} complexes are effective catalysts for oxyfunctionalization reactions, albeit with a substrate, benzoic acid, that contains a directing group that facilitates C−H activation. It is our hope that the mechanistic insights provided by this work will result in the development of new catalysts for the functionalization of C−H bonds with the Cp*Ir^{III} motif.

EXPERIMENTAL SECTION

Computational Studies. Theoretical calculations have been carried out using the Gaussian09[70] implementation of BP86 density functional theory.[71] All calculations were conducted with the same basis set combination. The Stuttgart-Dresden (SDD) relativistic effective core potential (RECP) basis set was used for iridium.[72,73] The LANL2DZ effective core potential and basis set (ECP)[74−76] was used for silver. The 6-31G(d,p) basis sets were used for all other atoms. Cartesian d functions were used throughout, that is, there are six angular basis functions per d function. All structures were fully optimized and analytical frequency calculations were performed on all structures to ensure either a zeroth-order saddle point (a local minimum) or a first-order saddle point (transition state: TS) was achieved. The minima associated with each transition state was determined by animation of the imaginary frequency and, if necessary, with intrinsic reaction coordinate (IRC) calculations. Solvation energies were computed geometries optimized in the gas phase using the SMD method,[77] with methanol as the solvent, as implemented in Gaussian 09. In this method an IEFPCM calculation is performed with radii and electrostatic terms from Truhlar and co-workers' SMD solvation model.[78] In this manuscript energies are reported in kcal/mol with gas phase energies in parentheses and solvation energies without parentheses.

ASSOCIATED CONTENT

Supporting Information

Experimental procedures for all catalytic reactions. Synthesis and characterization of all complexes. X-ray experimental procedures and data tables. Cartesian coordinates for all optimized complexes, as well as, the full Gaussian 09 reference. This material is available free of charge via the Internet at http://pubs.acs.org.

AUTHOR INFORMATION

Corresponding Author

*E-mail: eaison@ncsu.edu.

Notes

The authors declare no competing financial interest.

ACKNOWLEDGMENTS

This work was supported by the NSF as part of the Center for Enabling New Technologies through Catalysis (CENTC), CHE-0650456 and CHE-1205189. We also acknowledge the National Science Foundation via the CAREER Award (CHE-0955636) for funding. We thank Karen I. Goldberg, D. Michael Heinekey, William D. Jones, and Melanie S. Sanford for helpful discussions.

REFERENCES

(1) Nozawa, K.; Yamada, M.; Tsuda, Y.; Kawai, K. I.; Nakajima, S. *Chem. Pharm. Bull.* **1981**, *29*, 2689−2691.

(2) Kumagai, H.; Masuda, T.; Ohsono, M.; Hattori, S.; Naganawa, H.; Sawa, T.; Hamada, M.; Ishizuka, M.; Takeuchi, T. *J. Antibiot.* **1990**, *43*, 1505−1507.
(3) Korte, D. E.; Hegedus, L. S.; Wirth, R. K. *J. Org. Chem.* **1977**, *42*, 1329−1336.
(4) Barrero, A. F.; Oltra, J. E.; Herrador, M. M.; Cabrera, E.; Sanchez, J. F.; Quilez, J. F.; Rojas, F. J.; Reyes, J. F. *Tetrahedron* **1993**, *49*, 141−150.
(5) Qadeer, G.; Rama, N. H.; Fan, Z. J.; Liu, B.; Liu, X. F. *J. Braz. Chem. Soc.* **2007**, *18*, 1176−1182.
(6) Whyte, A. C.; Gloer, J. B.; Scott, J. A.; Malloch, D. *J. Nat. Prod.* **1996**, *59*, 765−769.
(7) Nakashima, T.; Hirano, S.; Agata, N.; Kumagai, H.; Isshiki, K.; Yoshioka, T.; Ishizuka, M.; Maeda, K.; Takeuchi, T. *J. Antibiot.* **1999**, *52*, 426−428.
(8) Pal, S.; Chatare, V.; Pal, M. *Curr. Org. Chem.* **2011**, *15*, 782−800.
(9) Mereyala, H. B.; Pathuri, G. *Synthesis (Stuttgart, Ger.)* **2006**, 2944−2950.
(10) Alami, M.; Provot, O.; Le Bras, G.; Hamze, A.; Messaoudi, S.; Le Calvez, P.-B.; Brion, J.-D. *Synthesis* **2008**, *2008*, 1607−1611.
(11) Tadd, A. C.; Fielding, M. R.; Willis, M. C. *Chem. Commun.* **2009**, 6744−6746.
(12) Mali, R. S.; Babu, K. N. *J. Org. Chem.* **1998**, *63*, 2488−2492.
(13) Rossi, R.; Carpita, A.; Bellina, F.; Stabile, P.; Mannina, L. *Tetrahedron* **2003**, *59*, 2067−2081.
(14) Ackermann, L.; Pospech, J.; Graczyk, K.; Rauch, K. *Org. Lett.* **2012**, *14*, 930−933.
(15) Knoelker, H.-J. *Curr. Org. Synth.* **2004**, *1*, 309−331.
(16) Rubin, M.; Sromek, A. W.; Gevorgyan, V. *Synlett* **2003**, 2265−2291.
(17) Wang, Z.-Q.; Liang, Y.; Lei, Y.; Zhou, M.-B.; Li, J.-H. *Chem. Commun.* **2009**, 5242−5244.
(18) Ackermann, L.; Pospech, J.; Graczyk, K.; Rauch, K. *Org. Lett.* **2012**, *14*, 930−933.
(19) Chinnagolla, R. K.; Jeganmohan, M. *Chem. Commun.* **2012**, *48*, 2030−2032.
(20) Ackermann, L. *Chem. Rev.* **2011**, *111*, 1315−1345.
(21) Ackermann, L.; Lygin, A. V.; Hofmann, N. *Org. Lett.* **2011**, *13*, 3278−3281.
(22) Ackermann, L.; Pospech, J. *Org. Lett.* **2011**, *13*, 4153−4155.
(23) Ackermann, L.; Vicente, R. *Top. Curr. Chem.* **2010**, *292*, 211−229.
(24) Ackermann, L.; Vicente, R.; Potukuchi, H. K.; Pirovano, V. *Org. Lett.* **2010**, *12*, 5032−5035.
(25) Deponti, M.; Kozhushkov, S. I.; Yufit, D. S.; Ackermann, L. *Org. Biomol. Chem.* **2013**, *11*, 142−148.
(26) Kornhaass, C.; Li, J.; Ackermann, L. *J. Org. Chem.* **2012**, *77*, 9190−9198.
(27) Kozhushkov, S. I.; Ackermann, L. *Chem. Sci.* **2013**, *4*, 886−896.
(28) Liu, W.; Ackermann, L. *Org. Lett.* **2013**, *15*, 3484−3486.
(29) Phani, K. N. Y.; Jeyachandran, R.; Ackermann, L. *J. Org. Chem.* **2013**, *78*, 4145−4152.
(30) Thirunavukkarasu, V. S.; Donati, M.; Ackermann, L. *Org. Lett.* **2012**, *14*, 3416−3419.
(31) Thirunavukkarasu, V. S.; Hubrich, J.; Ackermann, L. *Org. Lett.* **2012**, *14*, 4210−4213.
(32) Thirunavukkarasu, V. S.; Raghuvanshi, K.; Ackermann, L. *Org. Lett.* **2013**, *15*, 3286−3289.
(33) Hashimoto, Y.; Hirano, K.; Satoh, T.; Kakiuchi, F.; Miura, M. *Org. Lett.* **2012**, *14*, 2058−2061.
(34) Itoh, M.; Hashimoto, Y.; Hirano, K.; Satoh, T.; Miura, M. *J. Org. Chem.* **2013**, *78* (16), 8098−8104.
(35) Suzuki, C.; Hirano, K.; Satoh, T.; Miura, M. *Org. Lett.* **2013**, *15* (15), 3990−3993.
(36) Ueyama, T.; Mochida, S.; Fukutani, T.; Hirano, K.; Satoh, T.; Miura, M. *Org. Lett.* **2011**, *13*, 706−708.
(37) Itoh, M.; Hirano, K.; Satoh, T.; Shibata, Y.; Tanaka, K.; Miura, M. *J. Org. Chem.* **2013**, *78*, 1365−1370.
(38) Mochida, S.; Hirano, K.; Satoh, T.; Miura, M. *Org. Lett.* **2010**, *12*, 5776−5779.
(39) Mochida, S.; Hirano, K.; Satoh, T.; Miura, M. *J. Org. Chem.* **2011**, *76*, 3024−3033.
(40) Mochida, S.; Umeda, N.; Hirano, K.; Satoh, T.; Miura, M. *Chem. Lett.* **2010**, *39*, 744−746.
(41) Morimoto, K.; Hirano, K.; Satoh, T.; Miura, M. *J. Org. Chem.* **2011**, *76*, 9548−9551.
(42) Ueura, K.; Satoh, T.; Miura, M. *J. Org. Chem.* **2007**, *72*, 5362−5367.
(43) Engelman, K. L.; Feng, Y. E.; Ison, E. A. *Organometallics* **2011**, *30*, 4572−4577.
(44) Arndtsen, B. A.; Bergman, R. G. *Science* **1995**, *270*, 1970−1973.
(45) Blakemore, J. D.; Schley, N. D.; Balcells, D.; Hull, J. F.; Olack, G. W.; Incarvito, C. D.; Eisenstein, O.; Brudvig, G. W.; Crabtree, R. H. *J. Am. Chem. Soc.* **2010**, *132*, 16017−16029.
(46) Brewster, T. P.; Blakemore, J. D.; Schley, N. D.; Incarvito, C. D.; Hazari, N.; Brudvig, G. W.; Crabtree, R. H. *Organometallics* **2011**, *30*, 965−973.
(47) Hintermair, U.; Sheehan, S. W.; Parent, A. R.; Ess, D. H.; Richens, D. T.; Vaccaro, P. H.; Brudvig, G. W.; Crabtree, R. H. *J. Am. Chem. Soc.* **2013**, *135*, 10837−10851.
(48) Zhou, M.; Balcells, D.; Parent, A. R.; Crabtree, R. H.; Eisenstein, O. *ACS Catal.* **2012**, *2*, 208−218.
(49) Zhou, M.; Hintermair, U.; Hashiguchi, B. G.; Parent, A. R.; Hashmi, S. M.; Elimelech, M.; Periana, R. A.; Brudvig, G. W.; Crabtree, R. H. *Organometallics* **2013**, *32*, 957−965.
(50) Zhou, M.; Schley, N. D.; Crabtree, R. H. *J. Am. Chem. Soc.* **2010**, *132*, 12550−12551.
(51) Satoh, T.; Ueura, K.; Miura, M. *Pure Appl. Chem.* **2008**, *80*, 1127−1134.
(52) Wik, B. J.; Romming, C.; Tilset, M. *J. Mol. Catal. A: Chem.* **2002**, *189*, 23−32.
(53) Boutadla, Y.; Davies, D. L.; Jones, R. C.; Singh, K. *Chem.—Eur. J.* **2011**, *17*, 3438−3448.
(54) Davies, D. L.; Donald, S. M. A.; Al-Duaij, O.; Macgregor, S. A.; Polleth, M. *J. Am. Chem. Soc.* **2006**, *128*, 4210−4211.
(55) Davies, D. L.; Donald, S. M. A.; Macgregor, S. A. *J. Am. Chem. Soc.* **2005**, *127*, 13754−13755.
(56) Davies, D. L.; Macgregor, S. A.; Poblador-Bahamonde, A. I. *Dalton Trans.* **2010**, *39*, 10520−10527.
(57) Boutadla, Y.; Davies, D. L.; Macgregor, S. A.; Poblador-Bahamonde, A. I. *Dalton Trans.* **2009**, *0*, 5887−5893.
(58) Some evidence for decomposition was observed.
(59) Zhang, G.; Yang, L.; Wang, Y.; Xie, Y.; Huang, H. *J. Am. Chem. Soc.* **2013**, *135*, 8850−8853.
(60) Colby, D. A.; Bergman, R. G.; Ellman, J. A. *Chem. Rev.* **2010**, *110*, 624−655.
(61) Alberico, D.; Scott, M. E.; Lautens, M. *Chem. Rev.* **2007**, *107*, 174−238.
(62) Colby, D. A.; Tsai, A. S.; Bergman, R. G.; Ellman, J. A. *Acc. Chem. Res.* **2012**, *45*, 814−825.
(63) Guimond, N.; Gorelsky, S. I.; Fagnou, K. *J. Am. Chem. Soc.* **2011**, *133*, 6449−6457.
(64) Hyster, T. K.; Rovis, T. *J. Am. Chem. Soc.* **2010**, *132*, 10565−10569.
(65) An associative pathway was also considered, but this pathway led to intermediates that were significantly higher in energy (See Supportng Information).
(66) Ess, D. H.; Bischof, S. M.; Oxgaard, J.; Periana, R. A.; Goddard, W. A. *Organometallics* **2008**, *27*, 6440−6445.
(67) For these calculations $Ag_2(OAc)_2$ was used as a model for AgOAc as described in: Olson, L. P.; Whitcomb, D. R.; Rajeswaran, M.; Blanton, T. N.; Stwertka, B. J. *Chem. Mater.* **2006**, *18*, 1667−1674 ; Ag was modeled as Ag_2 by removing the OAc ligands from $Ag_2(OAc)_2$. Energies for **INT-9** were calculated as for example ΔG°_{rxn} (**INT-9**) = $\Delta G^\circ_{INT\text{-}9} + \Delta G^\circ_{Ag2} - (2\ \Delta G^\circ_{AgOAc} + \Delta G^\circ_{6})$. Ag_2 is clearly not an accurate representation for elemental Ag; as a result, the absolute values for ΔG°_{rxn} for steps involving AgOAc are too high and

represent an upper limit for the free energy. However, since this model was used for all steps involving AgOAc, the error associated with this model is systematic; therefore the relative trends in the energies are accurate..
(68) Grotjahn, D. B.; Brown, D. B.; Martin, J. K.; Marelius, D. C.; Abadjian, M.-C.; Tran, H. N.; Kalyuzhny, G.; Vecchio, K. S.; Specht, Z. G.; Cortes-Llamas, S. A.; Miranda-Soto, V.; van Niekerk, C.; Moore, C. E.; Rheingold, A. L. *J. Am. Chem. Soc.* **2011**, *133*, 19024−19027.
(69) Park-Gehrke, L. S.; Freudenthal, J.; Kaminsky, W.; Dipasquale, A. G.; Mayer, J. M. *Dalton Trans.* **2009**, 1972−1983.
(70) Frisch, G. W.; Trucks, G. W.; Schlegel, H. B.; et al. *Gaussian 09*, Revision A.02; Gaussian, Inc.: Wallingford, CT, 2009.
(71) Parr, R. G., Yang, W. *Density Functional Theory of Atoms and Molecules*; Oxford University Press: New York, 1989.
(72) Dolg, M.; Stoll, H.; Preuss, H.; Pitzer, R. M. *J. Phys. Chem.* **1993**, *97*, 5852−5859.
(73) Hehre, W. J.; Ditchfield, R.; Pople, J. A. *J. Chem. Phys.* **1972**, *56*, 2257−2261.
(74) Hay, P. J.; Wadt, W. R. *J. Chem. Phys.* **1985**, *82*, 270−283.
(75) Hay, P. J.; Wadt, W. R. *J. Chem. Phys.* **1985**, *82*, 299−310.
(76) Wadt, W. R.; Hay, P. J. *J. Chem. Phys.* **1985**, *82*, 284−298.
(77) Marenich, A. V.; Cramer, C. J.; Truhlar, D. G. *J. Phys. Chem. B* **2009**, *113*, 6378−6396.
(78) Tomasi, J.; Mennucci, B.; Cammi, R. *Chem. Rev.* **2005**, *105*, 2999−3093.